Polish J. of Environ. Stud. Vol. 19, No. 6 (2010), 1199-1211

Original Research

The Influence of Direct Non-Thermal Plasma Treatment on Particulate Matter (PM) and NO_x in the Exhaust of Marine Diesel Engines

Marcin Hołub[1]*, Stanisław Kalisiak[1], Tadeusz Borkowski[2]***, Jarosław Myśków[2]****, Ronny Brandenburg[3]*****

[1]Electrical Engineering Department, West Pomeranian University of Technology, Sikorskiego 37, 70-313 Szczecin, Poland
[2]Faculty of Marine Engineering, Maritime University of Szczecin, Wały Chrobrego 1-2, 70-500 Szczecin, Poland
[3]Leibniz Institute for Plasma Science and Technology (INP Greifswald), Felix-Hausdorff-Str. 2 17489 Greifswald, Germany

Received: 19 December 2009
Accepted: 25 May 2010

Abstract

Our paper discusses a combined approach to reduce NO_x and particulate matter (PM) emitted by medium-speed marine diesel engines using non-thermal plasma (NTP) reactors. The design of the employed reactor relies on dielectric barrier discharge consisting of 36 parallel electrode rods positioned as to allow for movement of gas stream through the assembly. The plasma was driven by a novel power supply based on a series-parallel resonance circuit topology, which permits high voltage and frequency operation. Early results from the implementation of the non-thermal plasma reactor in the exhaust duct of a test bench diesel engine demonstrate considerable improvement of gas composition and particulate matter emission at extremely low energy densities (up to 16 J/dm^3). The conversion of PM to gaseous SOF and soot is investigated and confirms that removal rate of unbalanced PM increases with a reactor's power. In addition, a partial oxidation of NO to higher nitride oxides (e.g. NO_2) is identified.

Keywords: non-thermal plasma, exhaust treatment, PM reduction, plasma exhaust treatment, marine diesel engine

Introduction

The International Maritime Organization (IMO) has recently adopted Annex VI of the International Convention for the Prevention of Pollution from Ships (MARPOL 73/78) [1]. In response, marine diesel manufacturers embarked on investigating a variety of methods with the aim to reduce NO_x emission to reasonably low levels relative to associated costs. Proposed techniques provide different degrees of effectiveness and entail a trade-off between NO_x emission and other exhaust gas components such as hydrocarbons, CO and, above all, particulate matter (PM). Current consensus is such that most convenient after-treatment emission reduction technologies ought be fitted externally to the engine and built into the exhaust gas system to keep the engine with rated performance optimized for low fuel consumption.

*e-mail: mholub@zut.edu.pl
**e-mail: kal@zut.edu.pl
***e-mail: tborkowski@am.szczecin.pl
****e-mail: jmyskow@am.szczecin.pl
*****e-mail: brandenburg@inp-greifswald.de

The combustion products of diesel fuel under stoichiometric conditions are carbon dioxide, water, and sulphur dioxide. Correspondingly, the components of incomplete combustion are: carbon monoxide, nitrogen oxides, partially oxidized hydrocarbons, and PM. Partially unburned and burned compounds are due to several factors influencing combustion, such as fuel spray and mixture formation, variable air-to-fuel ratio, and vicinity to the combustion chamber wall. The precise chemical composition depends on the temperature of the exhaust gas. Carbon-based primary particles usually amount to soot. The particulate mass emissions from diesel engines are typically 10-100 times higher than those from spark ignition engines [2, 3]. These products typically include various unsaturated hydrocarbons, particularly acetylene and its higher analogues, and polycyclic aromatic hydrocarbons (PAH), which are very small in size (<2 nm). It is widely accepted that soot particle formation is preceded by the presence of PAHs [4]. The particle surface growth and, consequently, the attachment of gas-phase species to the solid-phase material, leads to an increase of soot. Nevertheless, it is known that numerous particles remain fundamentally unaffected.

The particles vary in size with typical observed size-distribution between 10 and 1,000 nm in diameter. Aforementioned stages of particle generation and growth constitute the soot formation process. At each stage of the process oxidation can occur, where soot and its precursors are burned to form CO or CO_2. The eventual soot emission will depend on the balance between these processes – formation and burnout. The emitted soot is then subject to further mass accumulation by adsorption into the soot particle surface and condensation to form a new particle layer in the exhaust system channel. If the fuel contains sulphur, it is mostly oxidized to SO_2, but a small fraction is also oxidized to SO_3, which inserts particles with sulphuric acid and sulphates. The sulfuric acid/sulfate fraction is largely proportional to the fuel sulphur content. The fraction related to unburned fuel and lube oil – soluble organic fraction (SOF) – varies with engine design and operating conditions, and is highest at low engine loads when exhaust temperatures are low. Metal compounds in the fuel, especially low-grade cylinder or circulating lubricating oil, leads to small amounts of inorganic ash.

Particulate matter (PM) emission from diesel engines poses one of the biggest issues stemming from their operation, particularly due to the impact on the environment and human health. The health effect of soot particles is generally attributed to the organic fraction containing the aforementioned polycyclic aromatic hydrocarbons (PAHs) [5, 6]. The emitted particles may contain volatile and liquid constituents, which makes their chemical composition very heterogeneous. There is some evidence that chemical characteristics of PM vary with the source of emission and that the toxicological features and associated health side effects differ between dispersion sites. Comparison of direct toxicological parameters between PM fractions demonstrated higher toxicity for PM2.5 than the larger-size fractions – PM10 [7]. Similar effects concerning PM size but causing DNA damage when absorbed in soluble extracts were also reported [8]. The study confirmed that PM composition is more relevant than sheer PM mass in assessing health effects of harmful exhaust gases.

Diesel engine exhaust treatment with low temperature plasma reactors has been studied by many research groups in recent years as a potential lean exhaust after-treatment method [9]. Non-thermal plasma was shown to improve emissions of both NO_x and particulate matter (PM). The effective partial oxidation of NO to NO_2 in plasmas has been widely demonstrated [10]. Hydrocarbons (HC) such as C_3H_6 or CH_2O were found to lower the energy cost for oxidation of NO to NO_2, while the oxidation of SO_2 and acid products suppressed it [9, 11]. In particular, OH-radicals play an important role in the oxidation process. Moreover, Hammer [10] and McAdams [12] investigated plasma-enhanced and plasma-activated selective catalytic reduction (PE-SCR or PA-SCR) with relation to NO_x emission reduction. The combination of plasma and catalyst proved a promising combination, since NO_2 can be reduced at low catalyst temperatures (i.e. below 200ºC). What's more, hydrocarbons can be used as reductants for NO_x removal (so-called HC-SCR). It was also demonstrated that soot particles can be decomposed through non-thermal oxidation by means of active species and other plasma products, e.g. NO_2 [13]. In [14], a wall filter was directly combined with the plasma, leading to soot decomposition by oxidation via ozone and other oxygen species. In [15], diesel particulate filters (DPF) were shown to regenerate from collected PM via ozone injection and plasma desorption. It has been found that most of PM could be oxidized completely into gaseous products of CO and CO_2 under plasma discharge conditions given that process conditions are carefully adjusted [16]. The process is associated exclusively with residency time and very low NO concentrations. However, PM removal efficiency decreased significantly with an increase of energy density. When NO concentration becomes higher, it acts as a catalyst that accelerates PM oxidation [17].

Likewise, NO can be removed via reduction to N_2 and oxidation to NO_2, which is further reduced by PM or used to produce HNO_2 and HNO_3 [9, 18, 19]. In a scaled up system with the whole exhaust gas from diesel engine passing through the plasma reactor, the residency period was 17.0 ms and efficient PM removal was 42% [17]. In uneven dielectric barrier discharge (DBD) reactors a maximum reduction of 67% at 300 W energy injections was obtained [20]. Moreover, marine diesels pose a number of idiosyncratic problems as the design and operating conditions differ largely from the automotive and land-based industrial applications [21, 22, 26]. The main differences include power ratings, nominal rotational speed, or operation with lower grade distillate or heavy fuel oil feeding.

Today, the shipping market is dominated by highly efficient diesel engines which run on low-quality fuels and recover the exhaust gas heat by means of exhaust gas boilers. Increased thermal efficiency resulting from reduced

Table 1. Marine diesel engine specifications.

Type		Nominal rate			Emission
Designation	Manufacturer, type	Power [kW]	Speed [revs/min]	SFOC [g/kWh]	NO_x weighted [g/kWh]
Small ship main propulsion or generator sets	HCP SULZER, 6AL20/24 (4 stroke)	397	720	218	17.4*

*IMO limit (Tier 1), 12.1 g/kWh.

fuel consumption further decreases exhaust temperatures. Furthermore, present marine fuels available on the market contain high quantities of asphalt, sulphur, and ash that considerably contaminate the exhaust gas and thereby increase the risk of soot deposits on the internal exhaust system walls and steam boiler tubes. In recent years the tendency to foul (i.e. soot deposits) has increased and in some cases resulted in fires due to the use of low-grade fuel. In extreme cases, a soot fire can develop into a high-temperature iron fire in which the steam boiler itself burns [24].

Existing conventional filter technology (DPF) of PM removal is far from perfect and suffers a number of predicaments. Filters with rough mesh pass very fine particles, whereas fine mesh ones are easily choked by large particles. Where plate reactors based on DBD are used, the deposition of PM on the internal reactor's elements (plates, insulators, and electrodes) results in a significant pressure drop and, consequently, engine performance deterioration. PM deposition can take place despite the DBD reactor operation [25]. An approach to solve this problem has been undertaken by combining the plasma corona discharge and liquid bath [26].

There are only a few studies reported in the literature considering the effect of NTP on diesel exhaust emitted by a test bed engine under realistic conditions [21, 13]. The present contribution is an attempt at combined approach to reduce NO_x and PM discharged by a marine medium speed diesel engine by means of a dielectric barrier discharge reactor. A novel power supply is used, which enables high voltage and high frequency operation for optimized electrical power input into the plasma. First results from the implementation of a non-thermal plasma reactor in the exhaust of a diesel test bench engine are reported, with a focus on gas and PM composition at very low energy densities. The paper is outlined as follows. Section 2 introduces all essential details of the experimental set-up (test bed, plasma reactor, power supply, and analytics). Subsequently, a presentation of the experimental results follows with some general findings on reactor properties and the analysis of induced plasma chemistry. The paper ends with discussion of the effects on PM reduction and gives concluding remarks together with an outlook for future research.

Experimental Set-Up and Procedures

Engine Test Bed and Apparatus Set-Up

The experiment was set to examine a combined approach to reduce NO_x and PM from diesel exhaust relying on the application of non-thermal plasma (NTP). The NTP module was installed on a bypass channel (about 10% flow of main duct) of the main exhaust system of a marine diesel engine whose specification data is shown in Table 1. Test bench construction enabled direct exhaust stream exposure (main exhaust bypass) to a plasma reactor without

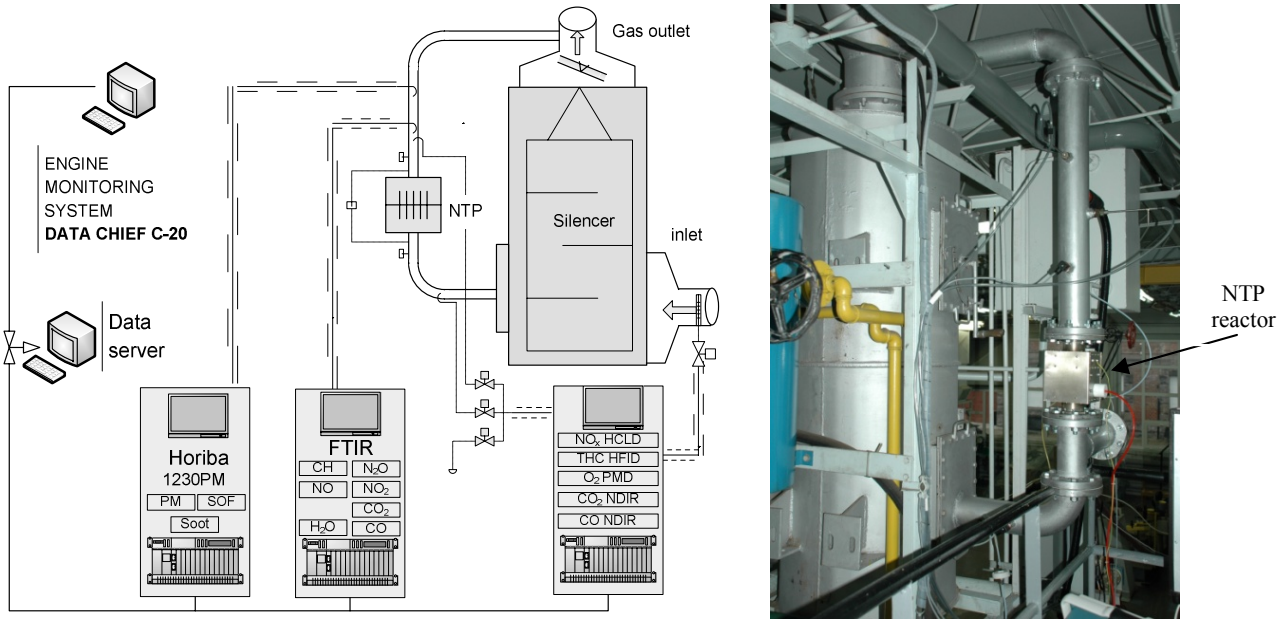

Fig. 1. Analyzer and acquisition system setup together with NTP unit in engine exhaust gas bypass.

Table 2. Fuel oil properties.

Determination			Test results
1	Density at 15ºC	kg/m^3	834.5
2	Viscosity at 40ºC	mm^2/s	2.55
3	C/H	%	85.80/14.10
4	N	%	0.02
5	O	%	0.05
6	S	%	0.02
7	CCR	%	0.01

any additional components (coolers, orifices) that could alter exhaust gas properties.

The experimental set up is shown in Fig. 1. The crucial gas component concentrations such as CO, CO_2, NO, NO_2, N_2O, NO_x, O_2, soot, soluble organic fraction (SOF, adsorbed hydrocarbons), and total PM were measured by state-of-the-art gas analyzers, namely Environment MIR FT – Fourier Transform Infrared Spectroscopy Multigaz Analyzer, HORIBA MEXA-1230PM, and AVL-CEB II Combustion Emission Bench. HORIBA MEXA-1230PM is a new monitoring system for PM emissions that enables separate analysis of soot and SOF in low mass levels. It consists of a diffusion charging (DC) detector with a dilution device for soot measurement, and two differential flame ionization detection (FID) detectors with separate sample lines maintained at 47ºC and 191ºC, respectively.

Throughout measurement trials the gas composition in the engine exhaust gas system was monitored by AVL-CEBII (after turbocharger and before the NTP reactor), while MIR FT(FTIR) and MEXA-1230PM were fitted at NTP reactor outlet. A set of thermocouples was used to estimate the temperature in the NTP module. The trial schedule allowed the reactor to heat up to reach stable conditions adequately for the engine exhaust system and outlet gas conditions. The NTP reactor temperature could not be adjusted as it depended on engine exhaust gas temperature. During engine tests it varied from 150ºC (idle) up to 350ºC under full engine load. This dependence was used to investigate the influence of process operating temperature on related oxidation processes.

During the measurement phase, the engine was in steady state of operation and all parameters were examined under two states: with and without NTP plasma operation (plasma on/off). Each plasma operation cycle was followed by idle run at the equal engine load. Exhaust gas velocity, temperature, and pressure in the NTP reactor's pipe were measured.

Likewise, gas velocity at the outlet of a reactor chamber was measured, allowing for gas stream speed estimation and effective gas residency time in plasma region. Gas temperature and pressure were recorded on the inlet and outlet sides of the reactor by means of an appropriate transducer acquisition system.

Emission measurements were carried out at steady-state engine operation. Sampling gas was distributed to all analyzers by means of heated, separate ducts. The measurement procedure was performed in accordance with Annex VI of Marpol 73/78 convention – with specification given in the IMO NO_x Technical Code and ISO-8178 standard. All tests were covered by test-cycle procedures D-2 and E-2. Both tests are characterized by constant (usually nominal) rotational engine speed and five (D-2) to four (E-2) effective torque settings. Single-engine effective load with nominal speed fulfills test-cycle requirements if rated torque falls into a specified range. During this experiment engine effective load was rated at 25% of nominal value where the highest PM emission was expected. The test was performed using selected marine distillate fuel DMX, fulfilling the ISO-8217 standard. A fuel sample was taken at the time of the trial for subsequent analysis in accordance to standard industry procedures. The appraisal results are given in Table 2.

All engine parameters were recorded continuously throughout trials, together with exhaust gas component concentrations recorded by means of measurement arrangements presented in Fig. 1 and summarized in Table 3.

Previous studies [27] have shown a very strong influence of operating conditions, independent of engine load, on PM emission. These may include, engine cooling water temperature, engine lubricating oil temperature, and charge air temperature. It should be spelled out that the above set of parameters in marine engines results from external systems and engine room installations, each of which has an independent control system. Measured engine system temperatures and pressure waveforms show a variable cyclic nature corresponding directly to the PM mechanism and emission. An example of such a process where the charge

Table 3. Basic engine parameters.

Engine data			Gaseous emission		
Effective power	kW	99.0	NO_x	g/h	1,729.0
Speed	rpm	720	CO	g/h	282.8
Turbocharger speed	krpm	15.1	HC	g/h	134.1
Fuel flow	kg/h	27.7	SO_2	g/h	5.5
Temp. intercooled air	ºC	42.0	CO_2	kg/h	87.1
Charge air pressure	kPa	295	Exhaust gas flow	kg/h	1,345

air temperature varies is shown in Fig. 2, with corresponding PM emission.

Another factor that seriously deforms the measurement of PM emissions in the exhaust gas of marine engines is the impact of the interior walls of the exhaust gas installation.

The transient nature of this process depends mainly on the engine effective load, which changes the temperature and velocity of the exhaust gas. Therefore, a fraction of measured PM is constantly changing, either increasing or decreasing, reflecting the current state of balance between the amount of PM particles settling and leaving the walls of exhaust outlet installation. Thus, a specific mode of PM measurements was devised that is characterized by brief on and off states of the NTP reactor power supply, achieving a significant reduction of the disruptive mechanism described.

NTP Reactor and Power Supply Unit

An NTP module for marine use requires a robust design, comparatively low voltage, low maintenance, and low energy consumption with easily scalable efficiency. The reactor construction was based on dielectric barrier discharge consisting of 36 parallel electrode rods, with the gas stream moving through the unit as described in [27].

A simplified cross-section of the designed NTP reactor (rod chamber) is depicted in Fig. 3. Outlined construction consists of three plates (numbered 1 to 3 on Fig. 3) that represent the construction base for low voltage rods (E) and quartz-glass dielectric barriers (I1). Plate 3 can be supplied with high-voltage, while the polarity of the supplied power can easily be reversed. Plates 2 and 3 are separated by dielectric I2. The arrows represent gas flow through a single tube.

There are two discharge zones: between plate 3 and barrier I1, and between the steel rod E and the barrier glass tube. The electronic power supply unit was characterized by a novel, series-parallel resonance circuit topology (SPRC) with ZCS (zero current switching) properties. Output voltage of the electronic power converter had the unique property of quasi-phase-mode voltage control. Additionally, this novel power supply topology enabled high voltage, high frequency operation.

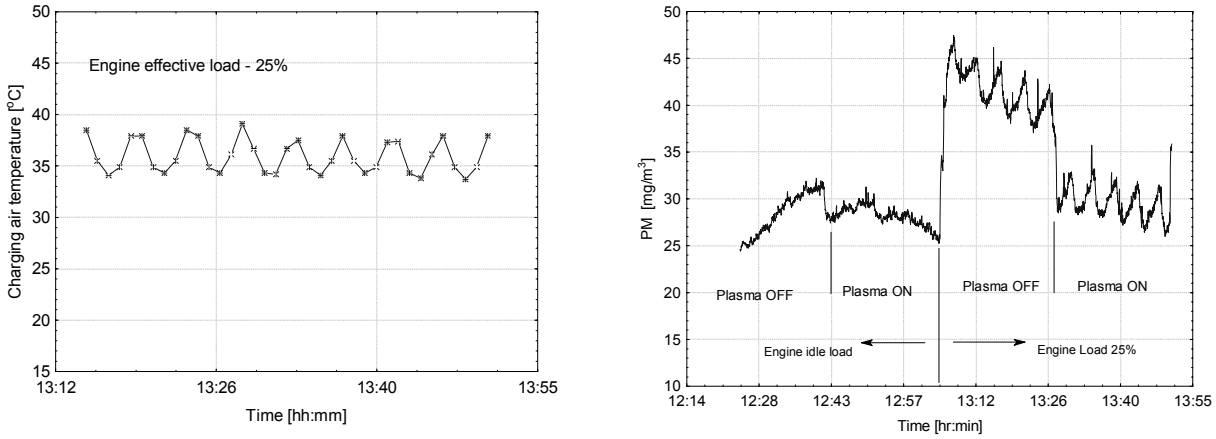

Fig. 2. Engine charge air temperature at 25% engine load and related PM concentration.

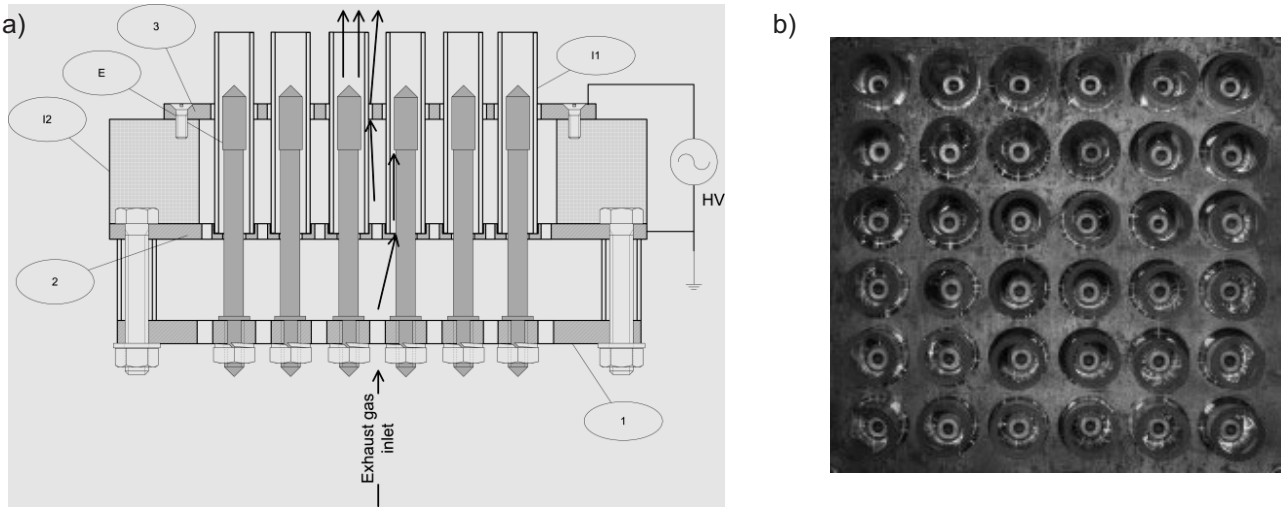

Fig. 3. Simplified cross-section of the DBD-reactor (a) and a photo with active plasma (b).
1-3 steel plates, I1 quartz-glass tubes, I2 dielectric, E – steel rods.

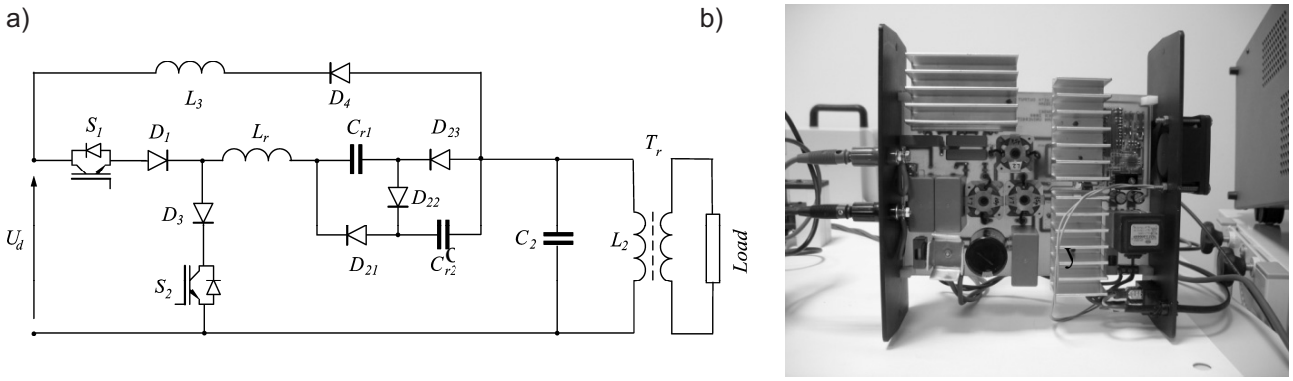

Fig. 4. a) Supply system topology, b) constructed prototype.

Topology of the converter is shown in Fig. 4a, while a constructed prototype is shown in Fig. 4b. In order to minimize S_2 voltage stress C_{r1}, C_{r2} based topology is introduced [28]. While charging through the $S_1 - D_1$ connection, both capacitors are charged serially, while during discharge through $D_3 - S_2$, they represent a parallel connection. In addition, over-voltage is reduced through $D_4 - L_3$ coupling to supply voltage source U_d.

During experiments peak-to-peak values of the AC reactor supply voltage were in the range between 12.3~13.3 kV. Voltage and current were measured at reactor terminals with a LeCroy PPE20kV high-voltage probe and via a CP031 hall effect-based current probe. Signals were recorded by means of WaveRunner 6100A digital oscilloscope. To measure the dissipated power or energy of the plasma the Lissajous-figure method was used [29, 30]. Therefore, the charge is measured via a capacitor between grounded electrode and grounding point. Plotting the charge as a function of the applied voltage results in a straight line if the plasma is off. When plasma ignites, a parallelogram is formed. The area of the parallelogram is the dissipated energy per high voltage period and thus a measure of the discharge power. Power supply input power was varied between 130W and 430W of active power in 7 steps for 10-20-minute intervals. Input power was stabilized and output frequency reached 25kHz.

Results and Discussion

NTP Reactor Conditions

Fig. 5a shows typical voltage and current curves for the DBD-reactor. Few examples of Lissajous-figures measured at different input power levels are shown in Fig. 5b. A typical parallelogram shape of the Lissajous-figures is witnessed. Fig. 6 shows the performance of the power supply characteristics. The reactor's power definition used throughout the text and figures ($Pe_{reactor}$ – power dissipated into the plasma) increases linearly with the input active power up to a value of about 270 W at about 430 W of input. Therefore, a maximum operational efficiency of about 62% was reached, calculated as follows:

$$\eta_{oper} = \frac{Pe_{reactor}}{Pe_{input}} \quad (1)$$

...where:
$Pe_{reactor}$ – power dissipated in plasma region [W]
Pe_{input} – supply input active power [W].

Fig. 6 shows that efficiency increases with input power reaching saturation at about 260 W reactor power. The plotted efficiency path of power supply and plasma reactor assembly is important for automatic control, particularly

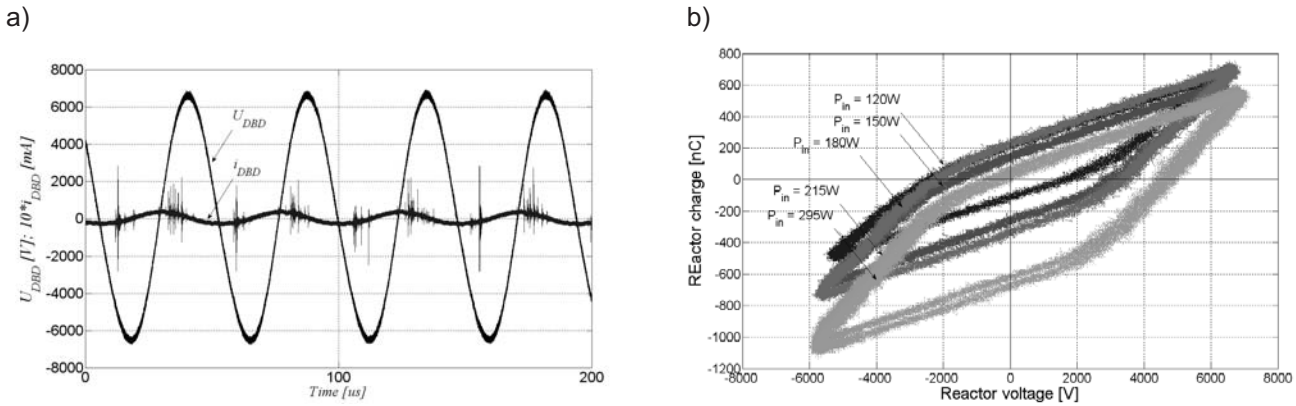

Fig. 5. a) Typical voltage and current diagram of the DBD-reactor, b) Lissajous-figures for different input power levels.

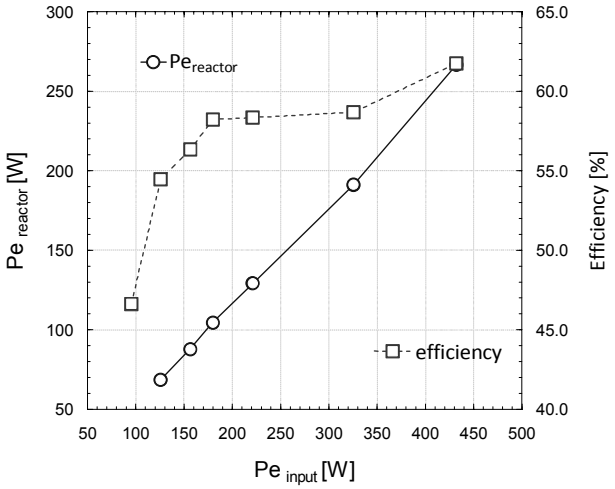

Fig. 6. Characteristic plasma input power supply with efficiency curve.

the initial part up the value of 170 W input active power, as opposed to the 170~320 W range where the path shows stable performance.

The engine and plasma reactor basic parameters are shown in Fig. 7. The rated torque (T_q) and fuel setting (H_{fuel}) during the measurement cycle are shown on the left-hand side, while NTP reactor gas temperature and pressure are shown on the corresponding right-hand side. Engine fuel setting (H_{fuel}) denotes the actual fuel rack position that is adjusted by the speed governor and is related to engine nominal load (H_{fuel}=100%). Operating the engine at a constant load to ensure stable plasma reactor conditions was one of the basic assumptions of the experiment. For this reason extra attention was given to control engine speed and torque. The quality of this process depended on external factors which, in turn, interfered with PM concentration analysis. Fig. 7 gives evidence that engine torque and fuel settings were constant during the test cycle.

Therefore, it is believed that the pressure ($p_{reactor}$) in the NTP reactor was also constant, while the temperature ($t_{reactor}$) increased up to 185ºC during the start phase of the cycle. The observed plasma reactor temperature fluctuation was due to external influence transferred from the engine charge air cooling system.

Parameters of the exhaust gas stream (velocity (v) and temperature) were determined through a Pitot tube located at the reactor's outlet. Estimated exhaust gas flow rate in the reactor was 44.2 Nm³/hr. Based on recorded gas composition and reactor structure single element assembly, the gas velocity ($v_{reactor}$) and residence time (t_{res}) in the discharge zone were calculated. The reactor's single element assembly with marked discharge region and distinctive dimensions used for calculation are schematically shown in Fig. 8.

Further gas properties in dependence to the energy dissipation in the plasma are presented in Fig. 9. The total reactor gas flow (V_{meas}) and gas flow velocity (v) were not significantly affected by the reactor's power. However, gas velocity inside the reactor's tubes slightly decreased with the reactor's power and consequently the residence time of the gas in discharge section increased up to about 0.66 ms. A significant difference in gas flow speed between the inlet of the reactor and individual reactor's elements indicates the possibility of significant efficiency improvement to the reactor design. For the current phase of the experiment, where the reactor was operated during low engine loads and low gas flows, current design meets the requirements.

In order to determine the quality of reactor operation, a continued assessment of the existing design of the energy index – specific energy density (*SED*) – was used:

$$SED = \frac{Pe_{reactor}}{V_{meas}} \quad [\mathrm{J/dm^3}] \tag{2}$$

...where: V_{meas} – gas flow [dm³/s].

As shown in Fig. 10a, the exhaust gas density (d_{gas} – at measurement conditions) stays constant for the range of the reactor's power. Consequently, the specific energy density increases linearly with the reactor's power. Another important factor for determining a practical solution of the reactor design is a drop of pressure inside the reactor. As men-

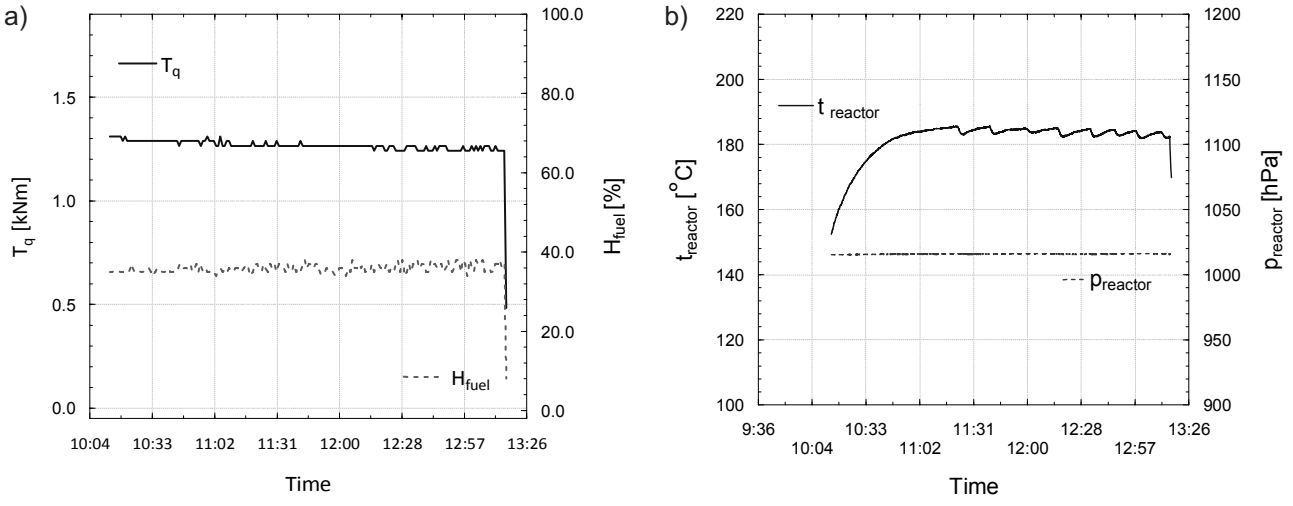

Fig. 7. Engine torque and fuel setting (a) and NTP reactor gas conditions (b) over a test cycle.

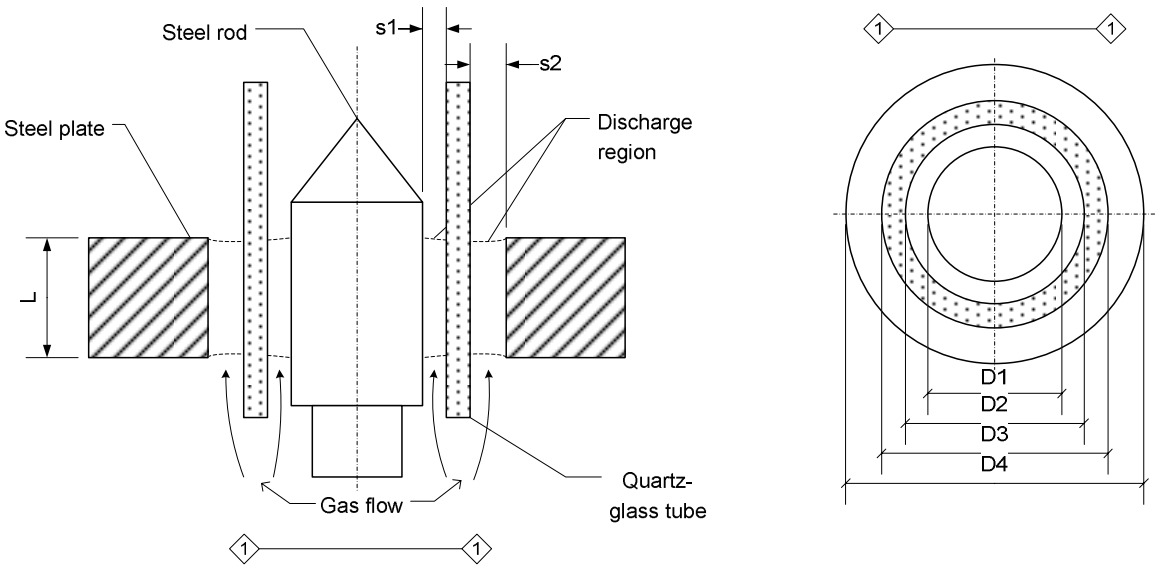

Fig. 8. Detailed reactor element assembly.

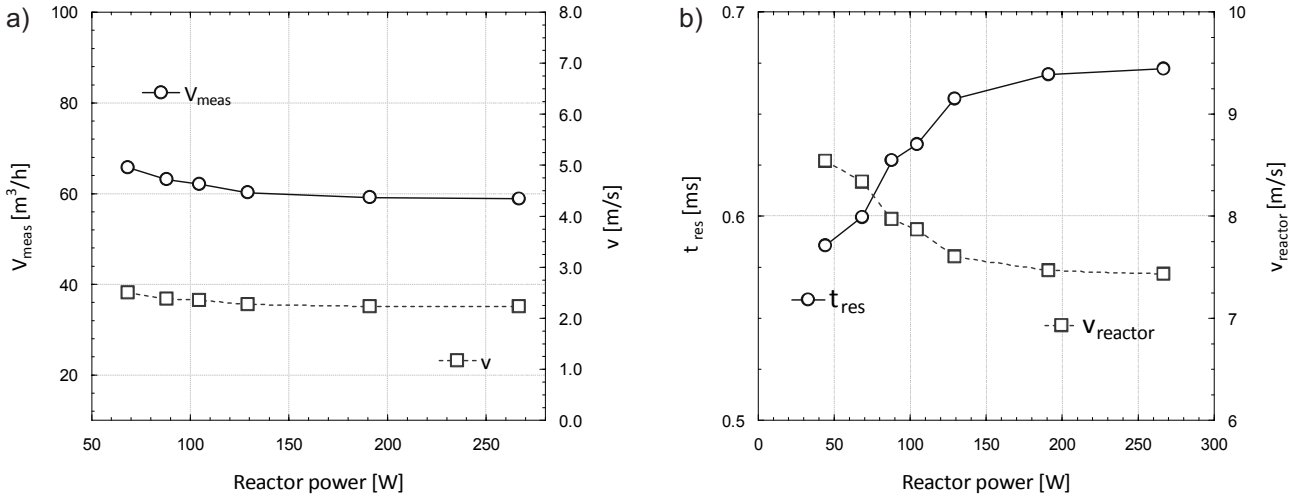

Fig. 9. NTP reactor inlet average gas flow and velocity (a); gas residence time and velocity in the NTP reactor (b).

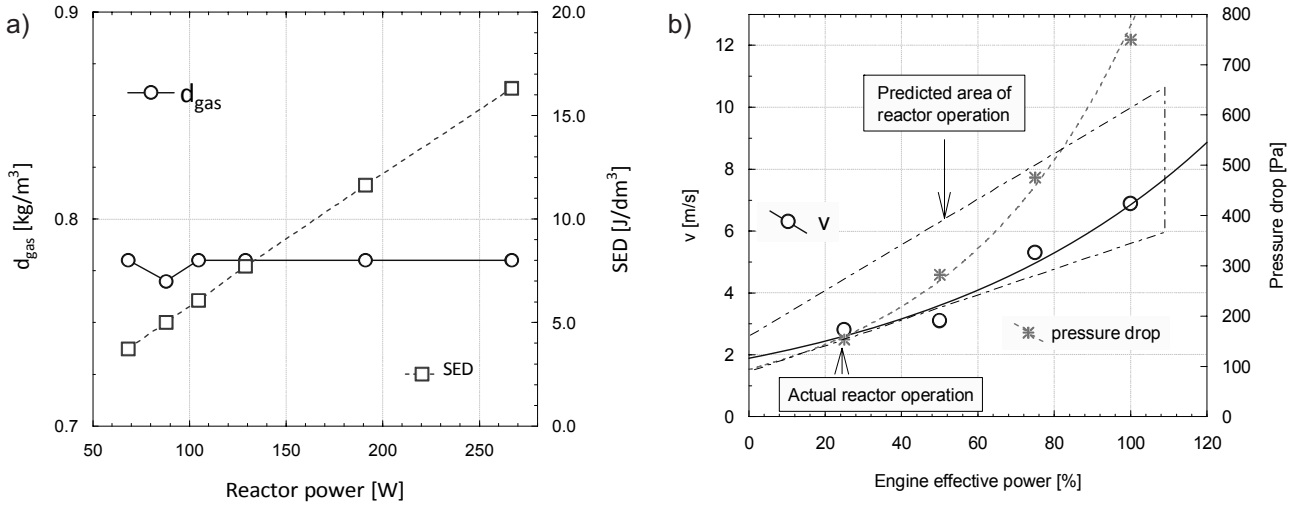

Fig. 10. Exhaust gas density and SED versus reactor power (a); gas velocity and pressure drop in reactor, under the full effective engine load range (b).

tioned earlier, marine reciprocating engines have a very low tolerance for increases in exhaust gas system back pressure. This is due to engine positioning in a vessel's engine room, for which a very long exhaust outlet system is necessary.

These factors force maintaining restrictively low pressure in the exhaust system and are subject to routine engine diagnoses. With this in mind in the current experiment, the pressure drop in plasma reactor was evaluated with anticipated growth for increases of engine load (Fig. 10b). The predicted values represent acceptable levels for marine engines.

NTP Reactor Performance Relative to Gas Composition and PM

The gas composition after engine turbocharger outlet (inlet to NTP rector) is shown in Fig. 11. The main components are CO_2, O_2 and H_2O, CO, NO_x and total hydro-carbons (THC). All emissions are approximately constant during the cycle, except for CO and NO_x,which were moderated through an imperfect charge air temperature control system.

The results of exhaust composition analysis after the NTP reactor (in outlet duct) are shown in Fig. 12. The plasma reactor was operated at input active power of 95~432 W, which corresponds to a residency time of about 0.59~0.67s and an SED of about 2.4~16.3 J/dm^3. Visibly, there is no significant change of C_xH_y concentration, but a slight increase of C_2H_4 is observed (Fig. 12b).

There is no total NO_x reduction due to plasma operation, but a fluctuating conversion of NO to NO_2 and N_2O due to oxidation processes induced by plasma is observed (notice the alternating local maxima and minima in the curves in Fig. 12a).

The NO_2 concentration increased significantly when plasma was switched on, reaching an apex at 130 ppm, as shown in Fig. 13a. This situation did not change even after a higher power was applied to the plasma. As an example, the density of propene as a function of reactor power is

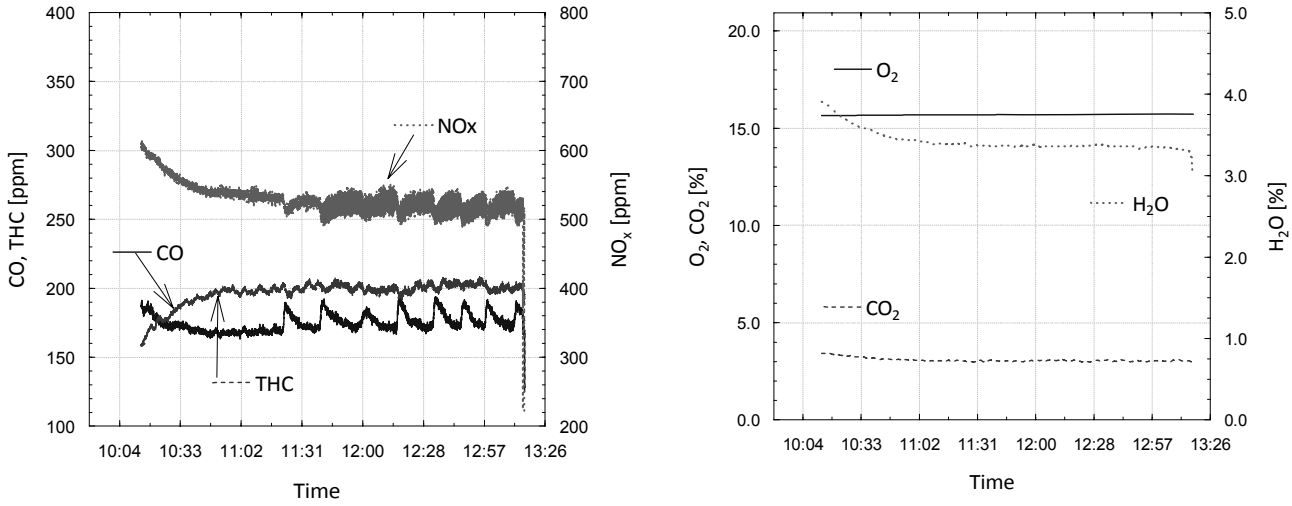

Fig. 11. Exhaust gas composition – measured at engine turbocharger outlet.

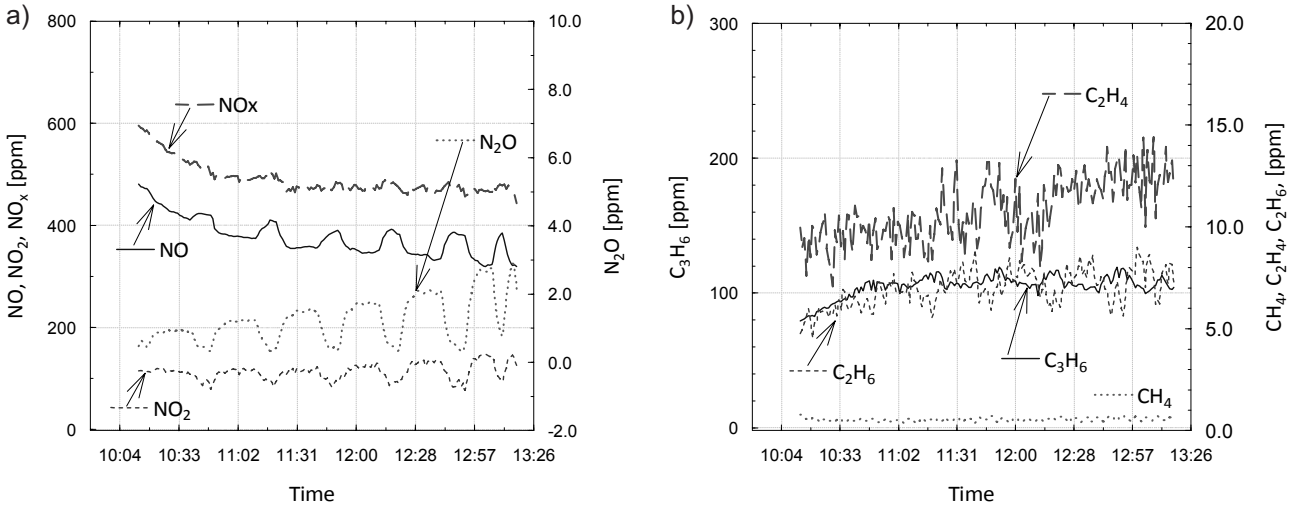

Fig. 12. Exhaust gas composition – measured at NTP reactor outlet.

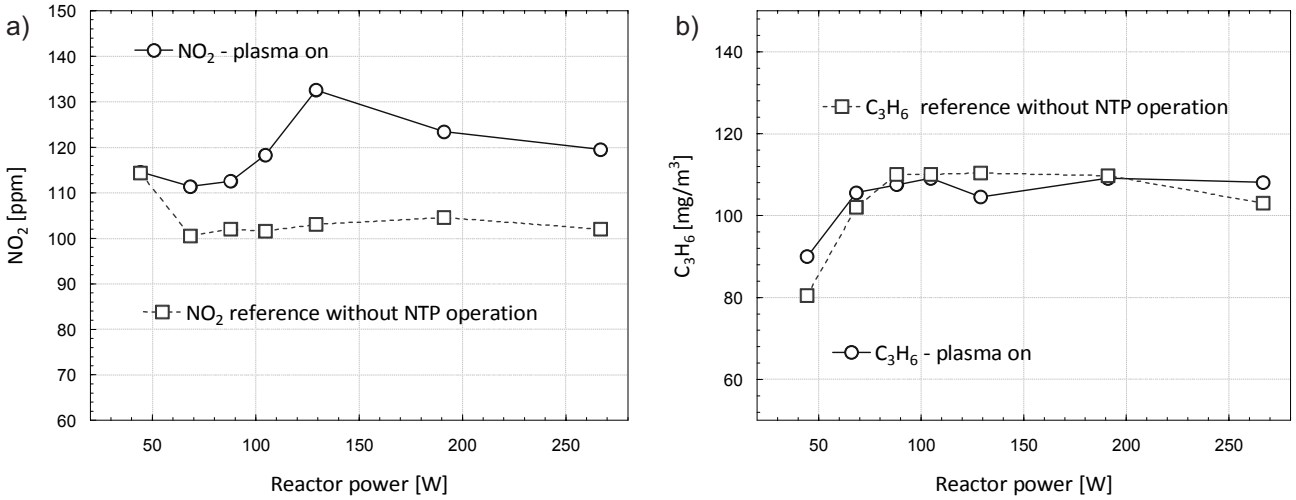

Fig. 13. Nitrogen dioxide and propene concentration versus reactor power.

shown in Fig. 13b. The conversion of propene is very low, since the energy density and residency time are moderate. Plasma treatment of NO by means of DBD predominantly results in conversion to NO_2. The NO removal rate increases due to reaction with propene. The reaction mechanism for the humid air-propene mixture is initiated by the creation of O and OH radicals that react with propene in a few different channels.

The effect of NTP treatment on soot and SOF is shown in Figs. 14, 15, and 16. From the diagram in Fig. 14 it can be ascertained that PM level concentration is quite unstable. The main constituent of PM is the SOF. For reasons previously described, there are divergent trends of changes in PM emission. Fig. 14 compares the change in PM concentration when reactor cyclic on/off mode was used (Fig. 14a) and when the reactor was switched off (Fig. 14b).

The variability of PM emission takes place in particular during engine load changes. During the whole test cycle soot content is rather stable, but decreases considerably for the last three reactor settings. However, for periods of reactor operation, soot level considerably increases, with the largest effect at the beginning of the cycle, even if energy density was very low ~3 J/dm^3. The SOF density has a positive trend throughout the cycle, regardless of the NTP reactor's state (on or off). In periods when plasma was operational, a considerable decrease in the SOF concentration was observed. The highest SOF reduction has been observed under ultimate reactor load – achieved in the seventh (short) stage.

A correlation between SOF decomposition and soot formation is clearly expressed in the diagrams in Fig. 15. Due to the soot-SOF concentration relation, total PM removal process has different effectiveness. In general, the PM removal rate in the NTP reactor is primarily based on the number of activated radicals. Carbon is removed via oxidation to CO and CO_2 [20]. Thus PM can deplete the radicals for NO to NO_2 conversion. Possible oxidants are atomic oxygen, OH and ozone, but the latter is not stable at temperatures above 50ºC. Very few studies on the mechanisms for PM removal using plasma focus on carbon soot removal [14].

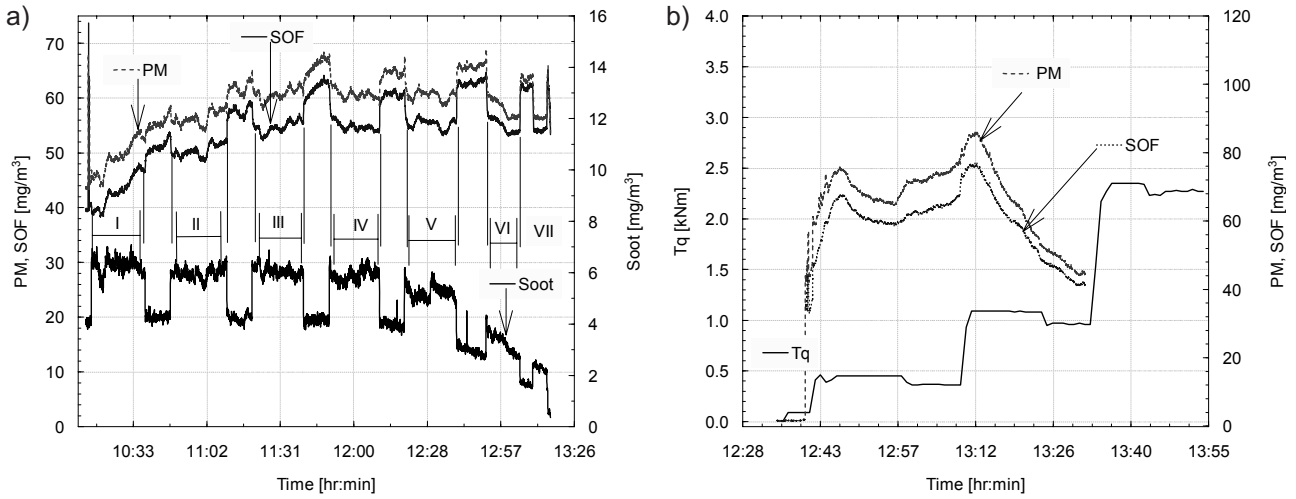

Fig. 14. Comparison of PM and related components concentrations with repeated reactor operation – cycles marked with I to VII (a) and under elevated engine load without reactor operation (b).

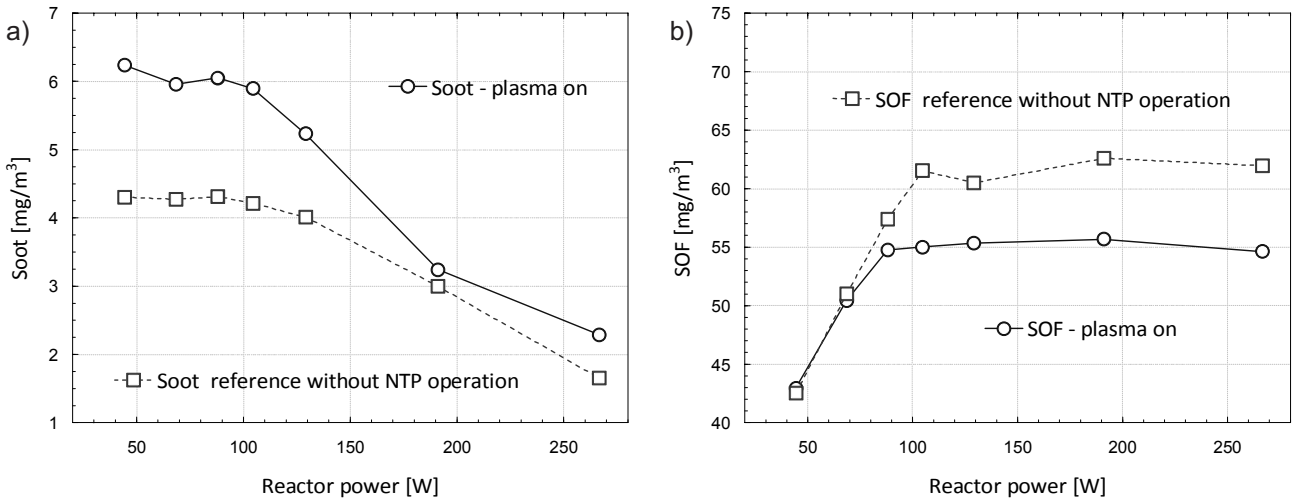

Fig. 15. Soot (a) and SOF (b) component concentrations as functions of reactor's power.

X-ray photon electron spectroscopy (XPS) on plasma-treated soot samples has confirmed that the decomposition process with ozone is a three-stage process. In the first (and relatively fast) step, HC in the soot particles are decomposed via ozone-oxidation. In the second step, a soot-oxygen complex is formed that leads to CO or CO_2 formation and thus carbon atom removal via ozone oxidation in the third step [31, 14] (i.e. PAH adsorbed on the soot can be removed, too). Another possibility to remove soot is via nitrogen oxides. In this case the soot-oxygen complex is formed via reaction with NO_2. The soot-oxygen complex is decomposed via ozone, which is an important requirement for the decomposition of soot. However, this reaction is much slower than the reaction via ozone at temperatures below 200ºC.

Based on the experiment presented here, a two-step process is proposed for the removal of marine diesel engine PM in the NTP. At first the SOF on the surface of the carbonaceous core of the PM (soot) are released due to the heat produced by NTP and then the released gaseous SOF are oxidized immediately by the oxidants in the plasma. Another possibility is the direct oxidation of the SOF on the soot-particles by active plasma species as described above. In any case, soot particles without SOF will remain and its density will be increased.

More studies are needed to clarify the processes in more detail. In assessing the NTP reactor's operation (Fig. 16b), it is necessary to note the significant increase in PM removal efficiency occurring at approximately 100 W of power corresponding to ~4.5 mg/min. The removal rate increases with reactor power, peaking at 6.5 mg/min of PM. At the same time there is a need to emphasize the negative effect on soot emission, which increases, reaching 2.7 mg/min at low reactor power and a value of 0.2 mg/min at highest reactor.

When assessing PM removal rate (Fig. 17) by using supply unit power (input active power), the efficiency is calculated as follows:

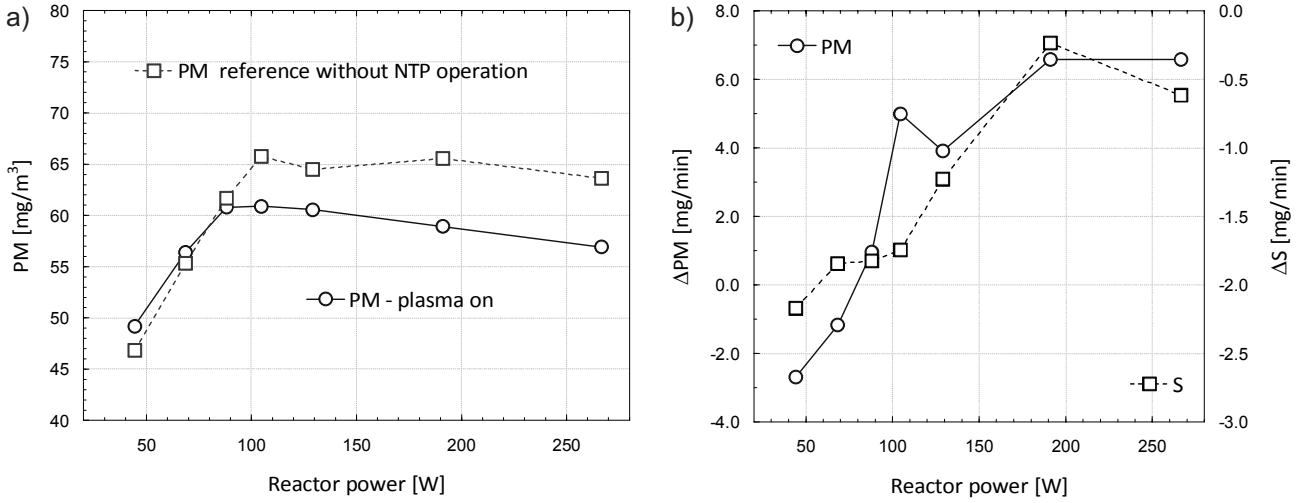

Fig. 16. Comparison of NTP reactor's efficiency in terms of PM concentration (a) and PM and soot mass flow rate removal (b).

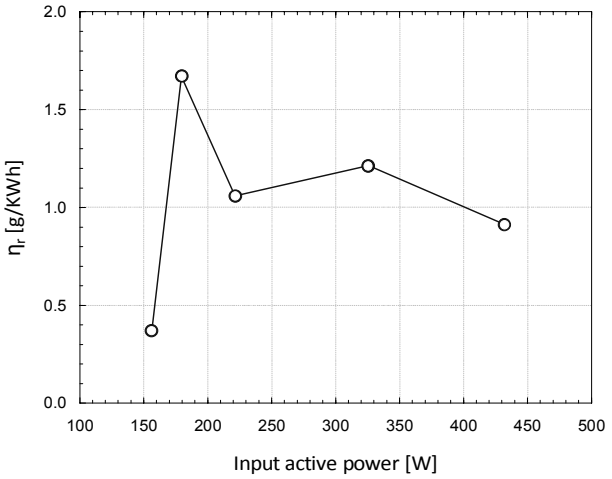

Fig. 17. PM removal efficiency associated with supply power.

$$\eta_r = \frac{\dot{m}_{PM_{off}} - \dot{m}_{PM_{on}}}{Pe_{input}} = \frac{\Delta\dot{m}_{PM}}{Pe_{input}} [g/kWh] \quad (3)$$

...where:
$\dot{m}_{PM_{off}}$ – PM mass flow rate without reactor operation [g/h]
$\dot{m}_{PM_{on}}$ – PM mass flow rate with reactor operation [g/h]
Pe_{input} – input active power [kW]

Summary and Outlook

An experimental study on the removal of particulate matter produced by a marine medium-speed diesel engine using non-thermal plasma was carried out. The plasma reactor design was based on a dielectric barrier discharge and driven with a novel power supply.

Proposed supply unit construction exhibits unique properties of phase-mode control of the output voltage, simple construction, and resonant operation (ZCS – zero current switching) independently of the system's load. Resonant operation also allows high efficiency rating of the system. Switch control signal length is fixed, and resonant frequency-based capacitor voltage waveform zero-crossing point (instead of distorted current) is used for phase delay and output voltage control properties.

First results on the implementation of a non-thermal plasma reactor in the exhaust of a diesel test bench engine show reasonable effects on gas and particulate matter composition. The NTP reactor design was characterized by a very low pressure drop.

The experiments were performed at very low energy densities of ~3 J/dm^3, up to substantial levels of energy density of ~16 J/dm^3. Significant effects on NO conversion as well as on PM conversion at realistic engine exhaust conditions (temperature and pressure) were noted. Removal rate of unbalanced PM amount was found, increasing from ~100 W of reactor's power to reach a maximum value of about 12% under 265 W, presented in Fig. 16a. Total PM removal efficiency was ~1.7 g/kWh at 180 W of input active power.

Partial oxidation of NO to higher nitride oxides (e.g. NO_2) was observed, as well as a conversion of PM particles to gaseous SOF and soot. Partial oxidation of NO was suggested as a conditioning for NO_x-catalyst based reduction processes at temperatures below 200ºC. Further investigations are necessary to understand the influence on PM, but the results suggest a two-stage process. Namely, the release of SOF by heat, followed by oxidation via reactive oxygen species in the plasma or the direct decomposition of the PAH on the SOF-particles.

Since the residence time in the reactor was short, no complete conversion was investigated. Future studies will necessitate advancements of plasma reactor designs and power supply topologies for improved power dissipation.

References

1. GOETZE H. J. Maritime Air Pollution Prevention Regulations from the View of a Classification Society, INTERNATIONAL COUNCIL ON COMBUSTION ENGINES, CIMAC Congress, Kyoto, pp. 187, **2004**.
2. KITTELSON D. B. Engines and nanoparticles: a review, Journal Aerosol Science, **29**, (5/6), 575, **1998**.
3. DAN Y., DENGSHAN G., GANG Y., XIANGLIN S., FAN G. An investigation of the treatment of particulate matter from gasoline engine exhaust using non-thermal plasma, Elsevier, Journal of Hazardous Materials **B127** 149, **2005**.
4. HEYWOOD J. B. Internal combustion engine fundamentals, McGraw-Hill, Inc. **1988**.
5. DE KOK T. M., HOGERVORST J. G, BRIEDE J. J., VAN HERWIJNEN M. H., MAAS L. M., MOONEN E. J., DRIECE H. A., KLEINJANS J. C. Genotoxicity and Physicochemical Characteristics of Traffic-Related Ambient Particulate Matter, Environmental and Molecular Mutagenesis **46**, 71, **2005**.
6. LUBITZ S., SCHOBER W., PUSCH G., EFFNER R., KLOPP N., BEHRENDT H., BUTERS J. T.M. Polycyclic Aromatic Hydrocarbons from Diesel Emissions Exert Proallergic Effects in Birch Pollen Allergic Individuals Through Enhanced Mediator Release from Basophiles, Wiley InterScience (www.interscience.wiley.com). DOI 10.1002/tox.20490, 20.April **2009**.
7. TAINIO M., TUOMISTO J. T., HÄNNINEN O., AARNIO P., KOISTINEN K. J., JANTUNEN M. J., PEKKANEN J. Health Effects Caused by Primary Fine Particulate Matter (PM2.5) Emitted from Buses in the Helsinki Metropolitan Area, Finland, Risk Analysis, **25**, (1), **2005**.
8. GUTIĔRREZ-CASTILLO M. E., ROUBICEK D. A., CEBRIÁN-GARCÍA M. E., DE VIZCAYA-RUÍZ A., SORDO-CEDEŃO M., OSTROSKY-WEGMAN P. Effect of Chemical Composition on the Induction of DNA Damage by Urban Airborne Particulate Matter, Environmental and Molecular Mutagenesis **47**, 199, **2006**.
9. CHAE J. O. Non-thermal plasma for diesel exhaust treatment, Elsevier, Journal of Electrostatics **57**, 251, **2003**.
10. HAMMER T. Non-thermal plasma application to the abatement of noxious emissions in automotive exhaust gases, Plasma Sources Sci. Technol. **11**, A196, **2002**.
11. PENETRANTE B., SCHULTHEIS S. E. Non-Thermal Plasma Techniques for Pollution Control: Part B – Electron Beam and Electrical Discharge Processing, Springer-Verlag, Berlin Heidelberg New York, **1993**.

12. MCADAMS R., BEECH P., SHAWCROSS J. T. Low temperature plasma assisted catalytic reduction of NO_x in simulated marine diesel exhaust, Plasma Chem. Plasma Process, **28**, 159, **2008**.
13. THOMAS S. E., MARTIN A.R., RAYBONE D., SHAWCROSS J.T., BEECH P., WHITEHEAD C.J. Non thermal plasma after-treatment of particulates-theoretical limits and impact on reactor design, SAE paper 2000-01-1926.
14. GRUNDMANN J., MÜLLER S, ZAHN R. J. Plasma Chem. Plasma Process. 25, **2005**.
15. OKUBO M., AITA N., KUROK T., YOSHIDA K., YAMAMOTO T. Total Diesel emission control using ozone injection and plasma desorption Plas. Chem. Plas. Proc. **28**, 173, **2008**.
16. YAO S., MADOKORO K. , FUSHIMI C., FUJIOKA Y. Experimental Investigation on Diesel PM Removal Using Uneven DBD Reactors, Wiley InterScience (www.interscience.wiley.com). DOI 10.1002/aic.11202, 14 May 14, **2007**.
17. YAO S., OKUMOTO M., YASHIMA T., SHIMOGAMI J., MADOKORO K., SUZUKI E. Pulsed Dielectric Barrier Discharge Reactor for Diesel Particulate Matter Removal, AIChE Journal, March **50**, (8), 1901, **2004**.
18. YAO S., OKUMOTO M., YASHIMA T., SHIMOGAMI J., MADOKORO K., SUZUKI E. Diesel PARTICULATE Matter and NO_x Removals Using a Pulsed Corona Surface Discharge, AIChE Journal, March. **50**, (3), 715, **2004**.
19. SONG C. L., BIN F., TAO Z. M., LI F. C., HUANG Q. F. Simultaneous removals of NO_x, HC and PM from diesel exhaust emissions by dielectric barrier discharges, Journal of Hazardous Materials, HAZMAT-9151; pp. 8, **2008**.
20. YAO S, FUSHIMI C., MADOKORO K., YAMADA K. Uneven cielectric barrier discharge reactors for diesel particulate matter removal, Plas. Chem. Plas. Proc. **26**, 481, **2006**.
21. MCADAMS R. Prospects for non-thermal atmospheric plasmas for pollution abatement, J. Phys. D: Appl. Phys. **34**, 2810, **2001**.
22. KOGELSCHATZ U. Dielectric-barrier Discharges: Their History, Discharge Physics, and Industrial Applications, Plasma Chemistry and Plasma Processing, **23**, (1), **2003**.
23. YOSHIOKA Y. Recent development in plasma De-NOx and PM (Particulate Matter) removal technologies from diesel exhaust gases, International Journal of Plasma Environment Science & Technology **1**, (2), 110, **2007**.
24. B&W MAN, Soot deposits and fires in exhaust gas boilers, Bulletin **2004**.
25. YAO S., KODAMA S., YAMAMOTO S., FUSHIMI C., MADOKORO K., CHIEKO M., FUJIOKA Y. Characterization of an uneven DBD reactor for diesel PM removal, ASIA-PACIFIC JOURNAL OF CHEMICAL ENGINEERING, Wiley InterScience (www.interscience.wiley.com) DOI:10.1002/apj.388. **2009**.
26. YOSHIOKA Y., TASHIRO Y., UEDA T., OTA Y., NAKANO K. Particulate Matter Removal from Diesel Exhaust Gases by a Combination of Corona Discharge and Water or Oil Bath, Plasma Processes Polymers, **3**, 713, **2006**.
27. BORKOWSKI T., MYŚKÓW J., HOŁUB M., KALISIAK S. Non-thermal plasma reactor use in marine diesel engine exhaust system, Journal of KONES Powertrain and Transport, PAN, Warsaw **15**, (3), 37, **2008**.
28. KALISIAK S., HOLUB M. A regenerative, passive snubber design for industrial IGBT power modules, PELINCEC 2005, 16-19 October, **2005**.
29. KRAUS M., ELIASSON B., KOGELSCHATZ U., WOKAUN A. CO_2 reforming of methane by the combination of dielectric-barrier discharges and catalysis, Phys. Chem. Chem. Phys., **3**, 294, **2001**.
30. WAGNER H. E., BRANDENBURG R., KOZLOV K.V., SONNENFELD A., MICHEL P., J.F. BEHNKE J. F. The barrier discharge: basic properties and applications to surface treatment, Vacuum, **71**, 417, **2003**.
31. KODAMA S., YAO S., YAMAMOTO S., MINE C., FUJIOKA Y. Oxidation mechanism of diesel particulate matter in plasma discharges, Chem. Lett. **38**, (1), 50, **2009**.